

Role of anion exchange membrane fouling in reverse electro dialysis using natural feed waters



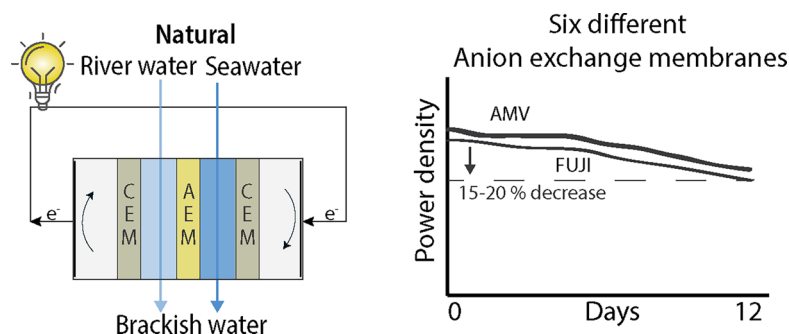
T. Rijnaarts^{a,b}, J. Moreno^{a,b}, M. Saakes^a, W.M. de Vos^b, K. Nijmeijer^{c,*}

^a Wetsus, European Centre of Excellence for Sustainable Water Technology, Oostergoweg 9, 8911 MA, Leeuwarden, the Netherlands

^b Membrane Science & Technology, University of Twente, P.O. Box 217, 7500 AE, Enschede, the Netherlands

^c Membrane Materials and Processes, Eindhoven University of Technology, P.O. Box 513, 5600 MB Eindhoven, the Netherlands

GRAPHICAL ABSTRACT



ARTICLE INFO

Keywords:

Anion exchange membranes
Fouling
Reverse electro dialysis
Natural water
Humic acids

ABSTRACT

Reverse electro dialysis (RED) is a process to harvest renewable energy from salinity gradients. Under lab conditions with artificial salt solutions, promising results have been achieved in recent years. However, in large scale industrial applications, natural waters are used and that poses challenges such as fouling. Fouling of anion exchange membranes (AEMs) by organic matter (e.g. humic acids) has been identified as a possible cause that lowers RED performance with natural waters. In this work, natural river and seawater at the Afsluitdijk (The Netherlands) are used to study the RED performance of six different AEMs. These AEMs are characterized before and after RED experiments with natural waters. The effect of natural fouling is found to be specific for each AEM and highly dependent on their respective chemistries and associated membrane properties. Firstly, aromatic AEMs with a low swelling degree showed a permselectivity decrease as well as membrane resistance increase. Secondly, aliphatic AEMs with a medium swelling degree experienced only a membrane resistance increase. Finally, only a decrease in permselectivity was observed for aliphatic AEMs with large swelling degrees. Subsequently, the effect of AEM fouling is compared to the observed decrease in RED performance and this shows that AEM fouling can only explain a minor part of the losses in open circuit voltage (OCV). The RED power densities dropped by 15–20% over 12 days, independent of the AEMs selected, while the reduced AEM performance could only explain 2–4% of this reduction in power density. This demonstrates that next to AEM fouling, also other factors, such as spacer fouling, are expected to be the dominant fouling mechanism, reducing the performance to a much larger extent.

* Corresponding author.

E-mail address: d.c.nijmeijer@tue.nl (K. Nijmeijer).

<https://doi.org/10.1016/j.colsurfa.2018.10.020>

Received 16 July 2018; Received in revised form 4 October 2018; Accepted 4 October 2018

Available online 09 October 2018

0927-7757/ © 2018 The Author(s). Published by Elsevier B.V. This is an open access article under the CC BY license (<http://creativecommons.org/licenses/by/4.0/>).

1. Introduction

Reverse electro dialysis (RED) is a membrane-based process to harvest renewable energy from natural salinity gradients. For RED, a membrane stack with alternating cation (CEMs) and anion exchange membranes (AEMs) is used. Feed waters with a difference in salinity (river and seawater for example) are fed to alternating stack compartments. In these RED systems, the salinity gradient between the two water sources generates an electromotive force (the open circuit voltage; OCV) and the charge-selective ion exchange membranes facilitate ionic transport (ionic current). In this way, the natural salinity gradient can be converted into electrical energy. Anticipated feed streams for this process are natural water sources with a salinity difference (e.g. river and seawater). In this case, this process uses renewable salinity gradient sources and can be part of the natural water cycle. In lab experiments, where artificial river and seawater were prepared using NaCl only, promising results have been obtained [1,2].

However, the use of real, natural water sources introduces challenges, such as the presence of divalent ions [3–5] membrane fouling [6,7], and spacer fouling [7,8] that decrease RED performance. In a RED pilot study in Harlingen, The Netherlands, Vermaas et al. investigated the effect of natural fouling using stacks with spacers or ridge-profiled membranes [7]. The study showed that the open circuit voltage decreased and the resistance increased, possibly due to organic matter fouling of the AEM. In addition, a substantial pressure drop along the feed water compartments, especially for the spacer-based stack, was observed, indicating fouling of the spacers. Others have also seen an increase in pressure drop over time due to fouling [8,9]. Cleaning spacers using bubbles decreased the pressure drop over the channel and allowed for operation at lower pressure drop over a prolonged time [8]. This clearly shows the relevance of spacer fouling. One cannot simply remove spacers (or profiles on membranes), since they are necessary in RED to allow for flow of water over the membranes surfaces. However, these spacers also are partially blocking the membrane surface and have a tendency to foul in natural water. This spacer fouling occurs simultaneous with fouling of the membranes and their surfaces, and it is complicated to discriminate between the different contributions of fouling. Indeed, the discussion on the relative importance of membrane versus spacer fouling is ongoing also for other membranes types, for example in spiral wound NF/RO membranes [10].

A fluorescence study on the surface of ion exchange membranes showed fouling of the membranes. Especially the surface of anion exchange membranes was affected by humic acid in the river water compartment [9]. Another study [11], performed in North Carolina, studied the effects of natural organic matter on RED performance in several natural salinity gradients. Their main conclusion was that natural organic matter in the river water decreased permselectivity, most likely, of the AEMs. The interaction between organic matter and AEMs was studied before using humic acids. Kobus and Heertjes [12] showed, using humic acid sorption experiments, a stoichiometric sorption of multivalent humic acids to the fixed charged groups in AEMs (shown schematically in Fig. 1), which they attributed mostly to the low-molecular weight fraction of humic acids.

Moreover, they found a clear increase in the specific membrane resistance due to the sorption of humic acids, with more sorption leading to a higher resistance. This experimental relationship is approximately linear with a slope of 1000–2000 Ω cm per fraction of total fixed charged groups in the AEM occupied by humic acids (i.e. how much of the Cl^- at the fixed charged groups are exchanged by humic acid), with the exact number depending on the type of membrane. In other words, there appears to be a stoichiometric occupation of the negative multivalent humic acids with the positive fixed charged groups in the AEM. This causes a decrease in accessible charged groups for ion exchange, which increases the resistance of the membrane. For permselectivity, Kobus and Heertjes observed a small decrease upon HA

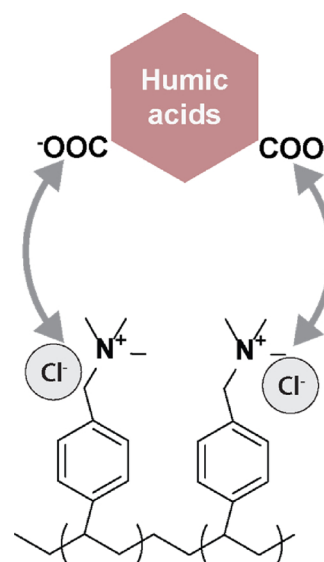


Fig. 1. Schematic mechanism of humic acid fouling of AEMs, with in this case aromatic backbone chemistry. Humic acids act as (large) multivalent anions, exchanging with counter ions (Cl^- in this case) and occupying fixed charged groups of the AEM [12].

adsorption, although the dependency is limited and values decrease from 97% to 85 and 95% for Ionac and Neosepta AEMs respectively.

Although very helpful, these results cannot be directly translated to natural fouling, as these fouling studies are accelerated by increasing the concentration of foulants to unrealistically high levels (1000 mg/L [12,13]), whereas in natural river water the dissolved organic carbon concentrations are usually only around 6 mg/L [8,11]. Moreover, many other types of fouling can occur in RED with natural waters, ranging from biofouling, to scaling and organic fouling by other organic compounds than humic acids.

Clearly, natural fouling in RED and the specific role of AEMs is not fully understood yet. Hence, in this work, the role of AEM fouling and the contribution of AEM fouling to the decrease in performance in RED is studied in detail using natural river and seawaters at the Afsluitdijk (NL). To this end, a systematic study is performed where the RED performance of six AEMs differing in chemistry and characteristics is investigated simultaneously for an extended period of 12 days. The AEMs are characterized before and after the experiments in natural waters are performed, to elucidate the contribution of AEM properties in relation to fouling. Finally, the effect of fouling on RED is compared at stack level (OCV, stack resistance and power density) and at AEM level (permselectivity and membrane resistance) to determine the role of AEM fouling under natural fouling conditions to the overall decrease in stack RED performance in natural waters.

2. Materials and methods

2.1. Membranes and chemicals

Homogeneous ion exchange membranes – Neosepta CMX and AMX (obtained from ASTOM Corp., Japan), Selemon AMV (obtained from Asahi Glass, Japan), Fuji V1, V2, V3A and V3B AEMs (received from FUJIFILM, The Netherlands) – were used. Humic acid sodium salt was purchased from Sigma-Aldrich. Sodium chloride (pharmaceutical grade) was kindly supplied by AkzoNobel (Hengelo, The Netherlands). Magnesium chloride hexahydrate and anhydrous calcium chloride were purchased from Sigma-Aldrich. Sodium sulfate (analytical grade) was purchased from Merck, The Netherlands. Potassium hexacyanoferrate (III) and potassium hexacyanoferrate (II) trihydrate were purchased from VWR Chemicals, The Netherlands.

Table 1
Qualitative description of AEMs and their supports used in this study.

AEM name	Backbone chemistry	Ion exchange capacity of polymer	Support thickness	Support porosity (open volume)
AMX	Aromatic	High	Thick > 100 μm	–
AMV	Aromatic	High	Thick > 100 μm	–
V1 (Type I)	Acrylamide [14]	Medium	Thick > 100 μm	High
V2	Acrylamide	Medium	Thin ~50 μm	Medium
V3A	Acrylamide	High	Thin ~50 μm	Medium
V3B	Acrylamide	High	Average ~80 μm	Low

Anion exchange membranes used in this study can be categorized in three different groups based on their polymer backbone chemistry and ion exchange capacity (IEC), as well as (estimated) thickness and porosity of the support. For clarity, Table 1 summarizes this in a qualitative way. In the results section, the experimentally determined qualitative values of the native membranes are given and discussed in relation to the change in these values upon fouling. All anion exchange membranes in this study are homogeneous membranes. Neosepta AMX and Selmion AMV are based on aromatic polymer backbones with low swelling and high charge densities, while the other AEMs (Fuji) are based on aliphatic acrylamide backbones with higher swelling. Fujifilm V1 (the commercial available Type I membrane) and V2 AEMs are prepared with the same recipe but on a different support, where the support of V2 is thinner and has a lower porosity than V1. Fuji V3A and V3B AEMs, however, share a recipe with a higher ion exchange capacity compared to recipe of V1 and V2. The difference between V3A and V3B is again the membrane support, where the support of V3B is thicker and has a lower porosity compared to the support of V3A. The most important difference between these membranes is the charge density, where V1/V2 have medium charge density and V3A/V3B have high charge density. A higher charge density in the polymer leads to larger swelling as well. The main discussion in this paper will be on the backbone chemistry in combination with the charge density of the membranes. These specifications are shown in Table 1.

2.2. Membrane characterization

Before each experiment, membranes were soaked for at least 24 h in 0.5 M NaCl to equilibrate them. The water content was measured by weighing the AEMs (~200 mg) after wetting in 0.5 M NaCl and after subsequent drying (in a vacuum oven at 30 °C overnight). The water content was calculated as the mass of sorbed water over the dry membrane weight. Membranes were characterized as single membranes in duplicate for resistance and permselectivity, according to procedures described earlier [5,15,16]. For area and specific membrane resistance measurements, a six-compartment cell was used with 0.5 M NaCl. For the membrane permselectivity, solutions of 0.1/0.5 M NaCl were used to measure the membrane potential. The measured potential, relative to the theoretical one as obtained from the Nernst equation, is reported as the membrane permselectivity. After RED operation with natural waters during 12 days, the same characterizations were performed again. For this, the fouled AEMs were immersed in 0.5 M NaCl for 24 h before the characterization measurements. Photographs of the fouled AEMs are shown in the Supplementary Information (SI 1).

The ion exchange capacity of clean AEMs (~200 mg) was determined by first exchanging the membranes to Cl^- form by soaking them twice in 100 mL of 3.0 M NaCl overnight. Then, after soaking thoroughly for 3–4 h with milliQ water to remove excess NaCl, the AEMs were placed in 100 mL of 1.0 M Na_2SO_4 . The sulfate solution was replaced twice and, after the AEMs were removed, the Cl^- content of the combined sulfate solutions was determined by AgNO_3 titration. The ion exchange capacity was calculated from the Cl^- content (in meq) over the dry AEM mass (g). The charge density (meq/g H_2O) can be calculated from the Cl^- content (in meq) over the mass of water in the AEM (g).

To determine the humic acid sorption of the different AEMs, clean AEMs were exposed to solutions containing humic acids. The AEMs (circles with diameter of 1.2 cm, weight 15–35 mg) were soaked for over 48 h in 30 ml artificial natural river water (6 mg/L (or ppm) humic acid, 30 mM NaCl, 5 mM MgCl_2 , 15 mM CaCl_2 [8]). Samples of the water were taken in duplicate before and after the experiment to determine the sorbed quantity of humic acids in the AEMs with UV–vis at 254 nm [11]. Control samples without AEMs were added to exclude (non-specific) sorption of humic acid on the petri dish. The fraction occupied by humic acids ($X_{\text{humic acid}}$) is calculated by dividing the equivalent of humic acids (grams of humic acids multiplied by their exchange capacity) by the equivalent of the membrane sample.

2.3. RED performance evaluation with natural water

Six cross-flow RED stacks ($10 \times 10 \text{ cm}^2$) supplied by REDstack BV (The Netherlands), were used in this experiment. Each stack was composed of 3 cell pairs, with 3 AEMs and 4 CEMs. In all cases, Neosepta CMX (ASTOM Corp., Japan) was used as CEM. Woven spacers of 485 μm (Sefar 06–700/53, Switzerland) with coated silicon rubber at the sides (Deukum, Germany) were used to keep the inter-membrane distance and to create the feed water compartments. Two titanium electrodes (mesh 1.7 m^2/m^2 , area 96.04 cm^2) with a ruthenium/iridium mixed metal oxide coating (Magneto Special Anodes BV, The Netherlands) were placed at both sides of the membrane pile. A solution of 0.05 M $\text{K}_3\text{Fe}(\text{CN})_6$, 0.05 M $\text{K}_4\text{Fe}(\text{CN})_6$ and 0.25 M NaCl in demineralized water was circulated through the electrolyte compartments by an adjustable peristaltic pump (Cole-Parmer, Masterflex L/S Digital drive, USA) with a flow rate of 150 ml/min. The electrolyte was kept under a slight overpressure of 0.3 bar to avoid bulging of the feed water compartments. Measurements were performed at 150 ml/min, which equals a linear flow velocity of 1.0 cm/s.

RED experiments were conducted at the REDstack Blue Energy research facility located at the Afsluitdijk, The Netherlands. This research facility uses natural feed waters, where a seawater intake is located at the Wadden Sea (Breezanddijk, The Netherlands) and a river water intake is located at the nearby fresh water lake (IJsselmeer, The Netherlands). For the RED experiments, both feed waters were pre-filtered through drum filters with a median pore diameter of 20 μm and, before the stacks, with an extra 5 μm filtration step to exclude fouling by larger particles. The ionic composition of the feed water was determined by ion chromatography (Compact IC Flex 930, Metrohm, The Netherlands). The conductivity and temperature of the influent were monitored and logged continuously during the experiment (Endress + Hauser Smartec-T, Germany). River and seawater ionic compositions, conductivities and temperatures are shown in Table 2, detailed values of conductivity and temperature over time are shown in SI 2. TOC values have been reported in previous work in similar conditions [8]. The experiment started on April 5, 2017 (day 0) and stopped on April 17, 2017 (day 12).

2.4. Electrochemical RED stack characterization

A chronopotentiometric series was applied using a potentiostat (Ivium Technologies, The Netherlands) every 30 min comprising of two

Table 2

Overview of averaged natural river water (RW) and seawater (SW) temperature, conductivity and ionic composition for the most common ions.

	Temperature (°C)	Conductivity (mS/cm)	Cations (mg/L)	Anions (mg/L)
RW	15.4 ± 1.8	0.55 ± 0.05	Na ⁺	81 ± 4
			Mg ²⁺	21 ± 2
			Ca ²⁺	59 ± 1
SW	15.5 ± 1.9	21.4 ± 7.7	Na ⁺	6856 ± 975
			Mg ²⁺	764 ± 105
			Ca ²⁺	637 ± 156
			Cl ⁻	121 ± 12
			SO ₄ ²⁻	55 ± 8
			Cl ⁻	11,725 ± 1698
			SO ₄ ²⁻	1531 ± 245

stages. The first stage was composed of a constant current density of 2.5 A/m² for 1380 s. The stack performance indicators were measured during the second stage with current density steps of 1.5 A/m², 2.5 A/m² and 3.5 A/m² established for 60 s to reach a constant voltage value. In between every step the current was set to zero for 60 s to measure the OCV. The stack area resistance was calculated from the steady state voltage during open circuit operation and during the stages with electrical current (1.5 A/m², 2.5 A/m² and 3.5 A/m²) using Ohm's law [5]. The gross power density was derived from the open circuit voltage (OCV), the stack area resistance and the total number of membranes according to:

$$P_{\text{gross}} = \frac{OCV^2}{4 \cdot R_{\text{stack}} \cdot N_m} \quad (1)$$

In which P_{gross} is the gross power density (W/m²), R_{stack} is the stack area resistance ($\Omega \text{ m}^2$) and N_m is the number of membranes in the stack (-). Data are compared with calculations based on the model from Veerman et al. with the specifications of the used stacks and membranes [17].

3. Results and discussion

3.1. AEM characterization

Prior to RED measurements, all AEMs are characterized to determine the differences between AEMs and to examine the effect of fouling after the RED experiments. Details regarding chemistries and supports are given in Table 1. The native AEM characteristics are shown in Table 3.

The most striking difference between the aliphatic (Fuji) and aromatic (AMX and AMV) membranes is their respective water content. Aromatic AEMs have a low water content and therefore high charge densities, resulting in high permselectivities. A downside is that this also leads to high area resistances for these membranes. On the other hand, the aliphatic Fuji membranes have higher water contents and therefore lower charge densities, which decreases their permselectivities. Moreover, these high water contents enable ion transport at relatively low membrane resistances. The differences between V1 and V2 are due to a different support, and causes V2, with a thinner support, to have a lower resistance as well as permselectivity. V3A has the same support as V2, but a chemistry with a higher IEC, which leads to a very high water content. The increase in resistance and permselectivity due

Table 3

Properties of studied AEMs. Duplicate (at least) measurements are performed for each membrane. Typical repeat errors for permselectivity are below 0.01.

AEM type	Charge density (meq/g H ₂ O)	Ion exchange capacity (meq/g dry AEM)	Perm-selectivity (-)	Area resistance ($\Omega \text{ cm}^2$)	Water content (g H ₂ O/g dry AEM)	Wet thickness (μm)
AMX	6.1 ± 0.0	1.4 ± 0.0	0.94	2.77 ± 0.07	0.23 ± 0.02	141 ± 6
AMV	10.1 ± 1.3	2.2 ± 0.3	0.95	2.44 ± 0.03	0.21 ± 0.03	110 ± 1
V1	3.3 ± 0.0	1.8 ± 0.0	0.90	1.05 ± 0.06	0.56 ± 0.09	139 ± 1
V2	3.4 ± 0.1	1.6 ± 0.1	0.86	0.67 ± 0.06	0.48 ± 0.11	53 ± 1
V3A	3.0 ± 0.2	2.2 ± 0.2	0.82	0.87 ± 0.02	0.71 ± 0.14	66 ± 1
V3B	2.9 ± 0.1	1.7 ± 0.0	0.87	1.36 ± 0.03	0.61 ± 0.10	84 ± 2

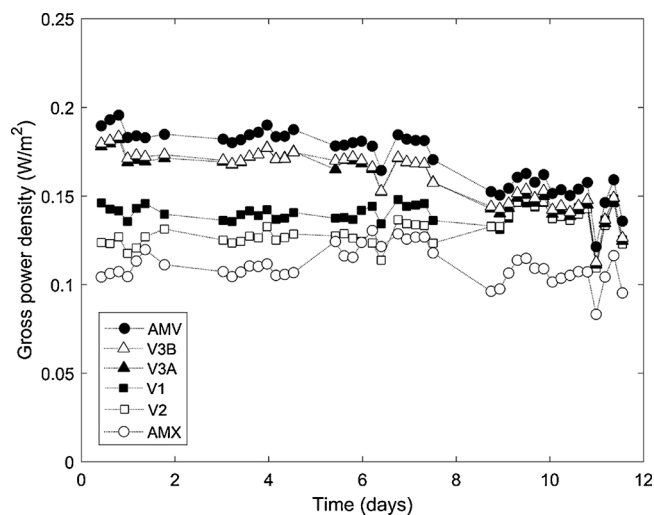


Fig. 2. Power densities (gross) as function of time for stacks equipped with studied AEMs. Lines are added to guide the eye.

to the thickness of the support is also visible when comparing V3A (thinner support) and V3B (thicker support). The recipe of V3A, with high IEC, is coated on a thicker and less porous support for AEM V3B.

3.2. RED stack experiment

The characterized AEMs were investigated on their RED performance in membrane stacks at the Afsluitdijk using natural waters (at stack level). In Fig. 2, the gross power density for each stack equipped with one of the six different AEMs is plotted against time. OCV and stack resistance graphs are shown in SI 3. During the first days of the experiment (day 1–day 7), the highest power density ($\sim 0.18 \text{ W/m}^2$) was achieved by the stack equipped with the Selemion AMV membrane, followed by FUJI V3B, V3A, V1 and V2. Similar values (0.17 W/m^2) have been found with natural water and similar spacer thicknesses using SK and SA membranes from PCA [11]. Membranes with the same chemistry, such as the V3A/V3B AEMs and the V1/V2 AEMs, perform almost identically in terms of gross power density, especially after longer operation times. The results will be further explained in Section 3.5, after addressing the effects of fouling on AEMs.

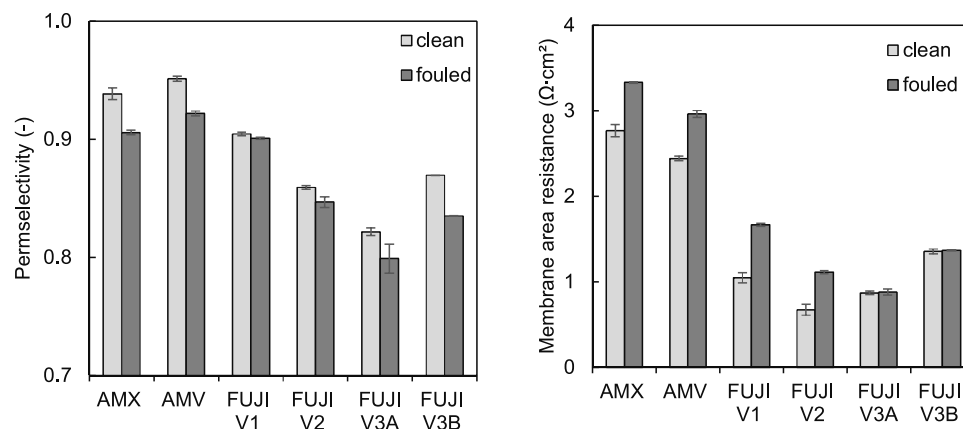


Fig. 3. Permeability (in 0.1/0.5 M NaCl) and membrane area resistance (in 0.5 M NaCl) for membranes in clean and fouled state. Error bars are error margins of duplicate measurements.

3.3. Fouled AEM characterization after RED fouling experiment

In Fig. 3, the membrane area resistance and permselectivities for all AEMs before and after RED operation are shown. Photographs of the fouled AEMs after RED measurements are shown in SI 1.

The effects of membrane fouling on the characteristics of the six different membranes can be subdivided into three groups (Fig. 3). Firstly, the aromatic AMX and AMV experience both a decrease in permselectivity (of 0.04) as well as an increase in resistance (of $0.5 \Omega \text{cm}^2$) due to fouling. These AEMs have an aromatic polymer backbone and a low water content (20–25%). Secondly, also V1 and V2 AEMs show similar behavior, namely a significant increase in resistance (of $0.4\text{--}0.6 \Omega \text{cm}^2$) while permselectivity is hardly affected. These membranes have a medium water content (40–60%). Thirdly, the membranes with a very high water content (over 60%), FUJI V3A and V3B AEMs, show similar behavior upon fouling as well. These membranes only show a small decrease in permselectivity (of 0.02–0.04) while the resistance of these membranes does not change.

From these experiments, one can conclude that the chemistry and especially the associated hydration of the membrane material is dominating the fouling behavior. Decreases in permselectivity due to organic matter in the river water have been observed in a previous study as well, where the use of natural river and seawater resulted in a permselectivity loss of ~ 0.12 for PC-SK/SA membranes [11]. This loss is however much higher than the loss observed in this study (0 up to 0.04 loss in permselectivity). These PCA membranes have a very low water content of 14 and 9% for the cation (SK) and anion (SA) exchange membrane respectively [18]. Although natural fouling is of course very much dependent on the specific feed water sources, this also confirms

that the effect of natural fouling on permselectivity is highly dependent on the membrane chemistry and especially the water content of the membrane.

3.4. Humic acid sorption study

To discuss the effect of natural fouling on membrane resistance, we need to include the sorption of model humic acids by these AEMs into account as well, since in previous work it was found that especially humic acid sorption plays a crucial role in natural fouling of AEMs [12]. To study the humic acid sorption systematically, a model humic acid river water solution is used (with humic acid concentration of 6 mg/L and cation concentrations representative for the Afsluitdijk [8]). From previous work, it is known that humic acids (as well as negative surfactants) can ion exchange with the Cl^- occupying the positive fixed charged groups in the AEM [12,19]. Moreover, there was a direct correlation between the quantity of humic acid occupying the fixed charged groups and an increase in membrane resistance [12].

In previous work, a very high concentration in the order of 1000 mg/L humic acids was used and, therefore, a high fraction (20 up to 95%) of the fixed charges of the membrane were occupied. In this study, we chose to use natural concentrations of 6 mg/L and - if one assumes an exchange capacity of humic acid of 3 eq/kg [20] - this results in an occupation of only 0.2–1.3% of the fixed charges of the AEMs. The amount of humic acid occupying the fixed membrane charges is different for the different AEMs. This is probably related to the accessibility of these fixed charges. If the AEM has a high water content, humic acids are able to diffuse into the AEM more easily and can thus occupy a larger fraction of the fixed charges. This is confirmed

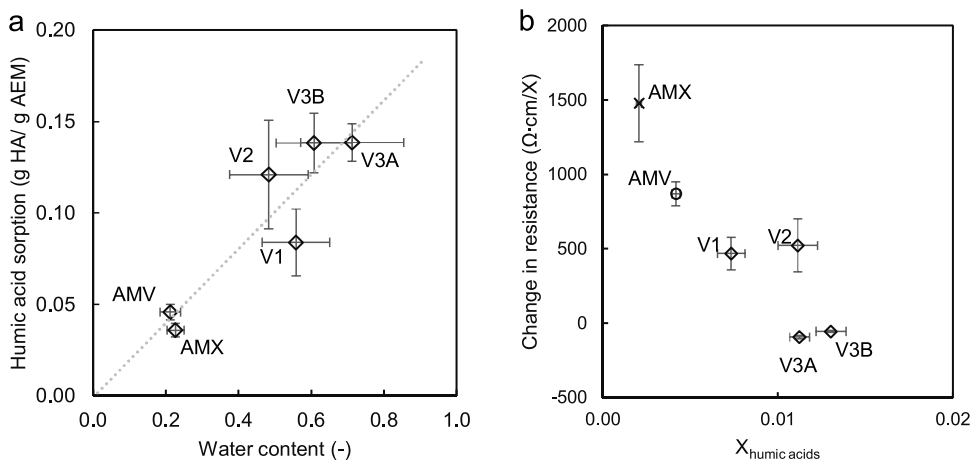


Fig. 4. Sorption of humic acid (a) in AEMs measured by UV-vis (at 254 nm) versus water content of the AEM. Change in membrane resistance (b) as function of humic acid occupation of the fixed membrane charges ($X_{\text{humic acids}}$). Error bars are standard deviations for sorption and water content (measurements performed in duplicate). The linear dashed line through the origin is meant to guide the eye.

in Fig. 4a, which shows the weight of sorbed humic acid per gram of membrane as a function of water content. There is a clear correlation between water content in the membrane and the adsorption of humic acids, where AEMs with a large water content are able to sorb substantially more humic acids per gram of membrane. A high water content in the AEM facilitates humic acid sorption.

Despite the low humic acid concentration, we find similar values for the resistance increase per humic acid occupied fixed charge ($\sim 1000 \Omega \text{ cm/eq HA}$) for AMV and AMX (see Fig. 4b). Fuji V1 and V2 have a resistance increase of $\sim 500 \Omega \text{ cm/eq HA}$, and both membrane V3A and V3B do not experience any membrane resistance increase. Also in this case the effect of membrane chemistry and water contents is clearly visible and distinguishes the three different types of behavior. This does not necessarily mean that if more humic acids are occupying fixed charges, the membrane resistance increases. That could be tested with different concentrations of humic acids for the same membrane. It means that the effect of humic acids occupying fixed charged groups on the membrane resistance is different for each membrane chemistry.

3.5. AEM fouling influence on stack performance

The decrease in RED performance due to the occurrence of natural fouling between clean (day 1) and fouled (day 12) membranes, investigated in Section 3.2, is visible as a decrease in OCV. Simultaneously, the change in permselectivity (before and after the RED experiment) of the membranes used in this experiment during 12 days can also be used to calculate the losses in RED performance specifically due to membrane fouling. In other words, the OCV loss of the stack includes all possible fouling occurring and leading to a reduction in performance, while calculation of the OCV loss based on the change in membrane permselectivity isolates the contribution of the change in membrane properties to the fouling from the other possible

contributions. The model of Veerman et al., which was validated for earlier experiments, is used to calculate the contribution of the change in properties of the AEMs upon fouling [17]. In Fig. 5a, the calculated effect of permselectivity of the AEM on stack OCV is shown, compared to the OCV data obtained from fouling experiments with the RED stacks.

The decrease in measured OCVs at the stack level is always significantly higher (5–9%) than the calculated values (1–2%) based on a change in AEM properties only (so any changes due to potential fouling of the CMX membranes are not included in this calculation). These data suggest that about only 20% of the total stack OCV loss is caused by changes in AEM properties. The remaining 80% of the OCV loss stems from other effects of fouling. As the feed water composition (tidal dynamics and presence of divalent ions) as well as the water temperature do not change significantly over time (shown in SI 2), examples of such foulants are organic matter as well as particles that can pass the pre-treatment. Both cause fouling on the membranes, but especially on the spacers as well [21]. Fouling of spacers can cause decreased flow distributions and local stagnant zones in channels, which lead to decreased OCVs due to lack of replenishment of solution at the membrane surface [22]. Therefore, the effective salinity gradient is decreased. Based on our results, this seems the dominant effect for the reduced OCV, while the effect of a change in AEM properties due to fouling [11,12] is less significant.

In Fig. 5b, the resistance change on stack level is shown and compared with the calculated effect of the change in AEM properties due to fouling. The calculated stack resistances based on the AEM resistances show no (V3A and V3B) or only a slight increase (AMV, AMX, V1 and V2). This is caused by the fact that the river water compartment comprises 90% of the total stack resistance, whereas the resistance of the AEM is of minor importance and comprises only 3–4%. The experimentally determined changes in resistance match the calculated values

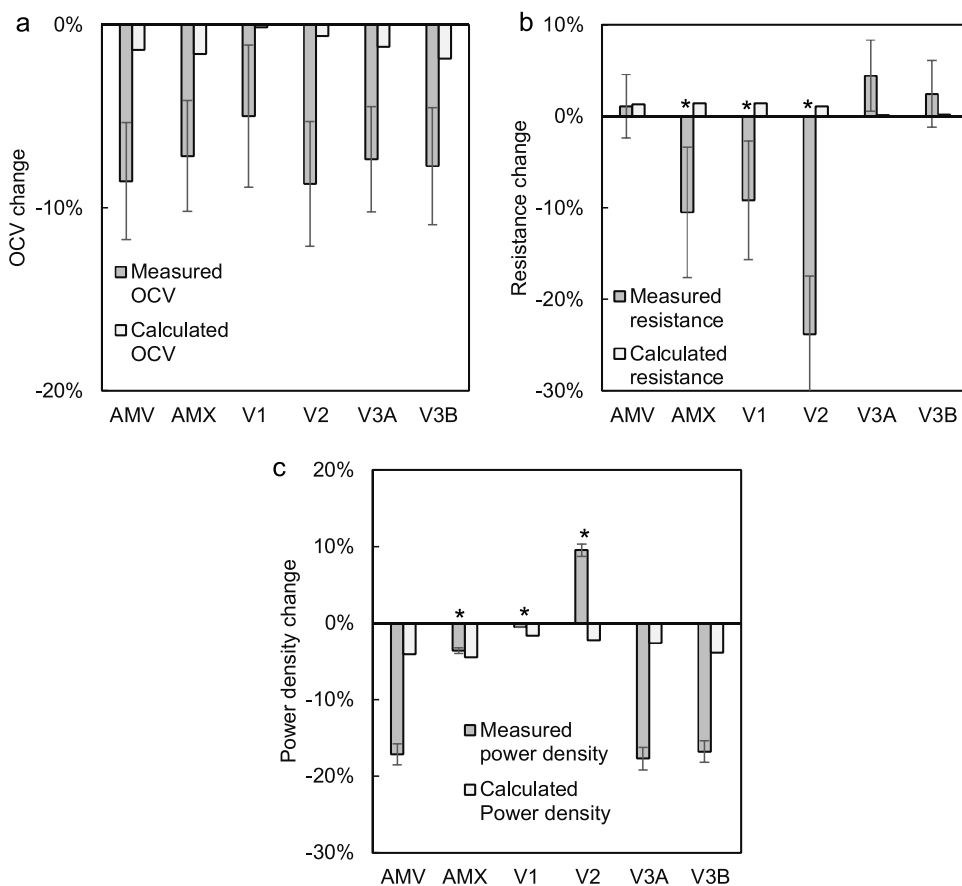


Fig. 5. Measured and calculated change from the average of day 12 compared to day 1, relative to day 1, for all AEMs in OCV (a), stack resistance (b) and power densities (c). Measured values are based on stack data at day 1 and day 12, calculated values are based on RED calculations with AEM permselectivity and resistance before and after RED experiments. * indicates resistances and power density measurements affected by bubbles in the spacers, these are therefore not representative.

reasonably well, taking into account the error bars, except for the measurements marked with * in Fig. 5 (AMX, V1, V2). In these cases, experimental resistances strongly decrease over time, which may seem counter-intuitive. This decrease is however, the consequence of air bubbles present in the stack and trapped in the spacer filaments that slowly disappear over time [8]. For this reason, the resistance and subsequent power density data are not representative. However, the membrane fouling data, as discussed in Section 3.3, are not affected since the membranes were still in contact with natural waters (see SI 1 for fouled AEM photographs). The OCVs are not affected as well, since these are not surface area dependent and bubbles do not decrease the salinity gradient [8]. Hence, OCVs and membrane fouling data are considered relevant, but stack resistance and power density data for the stacks equipped with AMX, V1 and V2 are less representative.

Finally, the experimental and theoretical effect of fouling on power densities is shown in Fig. 5c. The calculated power densities based on a change in AEM properties due to fouling, show only minor decreases of 2–4%. For the measured power densities, however, a clear decrease of 15–20% is observed for all stacks (excluding membrane stacks marked with *). These decreases are independent of the studied AEM, showing the minor contribution of AEM fouling to the decrease in stack performance. This again suggests severe fouling elsewhere in the stacks, i.e. in the spacers, as discussed before [10]. Alternatively, fouling of CEMs could contribute to a decrease in power density, however, it was shown that CEMs foul less compared to AEMs [7,13].

4. Conclusions

In this study the role of AEM fouling and the specific contribution of this AEM fouling to the decrease in total performance in RED is studied in detail using natural river and seawaters at the Afsluitdijk (NL). Depending on the membrane chemistry and the water contents, aromatic AEMs with low water content are affected negatively on both their permselectivity as well as their resistance. For the aliphatic AEMs with medium water content only membrane resistance decreases whereas for aliphatic AEMs with high water content mostly permselectivity is decreased.

The largest decrease in RED power density does not come from AEM fouling, which causes only a loss of 2–4% of a total loss of 15–20% during the operational period of 12 days. The major cause for fouling is fouling of the spacers in the fluid compartments, which disturbs flow distributions leading to lower OCVs. At the same time, stack resistances are hardly affected.

Author contributions

T.R., J.M., M.S., W.M. de V. and K.N. conceived the stack experiments. T.R. performed the humic acid experiments and membrane characterizations. J.M. performed the stack experiments. T.R., J.M., W.M. de V and K.N. analyzed and discussed the stack and membrane data. T.R. and J.M. wrote the paper and all authors reviewed the paper.

Declarations of interest

None.

Acknowledgements

This work was performed in the cooperation framework of Wetsus, European Centre of Excellence for Sustainable Water Technology

(www.wetsus.eu). Wetsus is co-funded by the Dutch Ministry of Economic Affairs and Ministry of Infrastructure and Environment, the Province of Fryslân, and the Northern Netherlands Provinces. The authors would like to sincerely thank the participants of the “Blue Energy” research theme for the strong collaboration, the many fruitful discussions and the financial support.

Appendix A. Supplementary data

Supplementary material related to this article can be found, in the online version, at doi:<https://doi.org/10.1016/j.colsurfa.2018.10.020>.

References

- [1] D.A. Vermaas, M. Saakes, K. Nijmeijer, Doubled power density from salinity gradients at reduced intermembrane distance, *Environ. Sci. Technol.* 45 (2011) 7089–7095.
- [2] J. Moreno, E. Slouwerhof, D.A. Vermaas, M. Saakes, K. Nijmeijer, The breathing cell: cyclic intermembrane distance variation in reverse electrodialysis, *Environ. Sci. Technol.* 50 (2016) 11386–11393.
- [3] J.W. Post, H.V.M. Hamelers, C.J.N. Buisman, Influence of multivalent ions on power production from mixing salt and fresh water with a reverse electrodialysis system, *J. Membr. Sci.* 330 (2009) 65–72.
- [4] D.A. Vermaas, J. Veerman, M. Saakes, K. Nijmeijer, Influence of multivalent ions on renewable energy generation in reverse electrodialysis, *Energy Environ. Sci.* 7 (2014) 1434–1445.
- [5] T. Rijnaarts, E. Huerta, W. van Baak, K. Nijmeijer, Effect of divalent cations on RED performance and cation exchange membrane selection to enhance power densities, *Environ. Sci. Technol.* 51 (21) (2017) 13028–13035.
- [6] W. Guo, H.-H. Ngo, J. Li, A mini-review on membrane fouling, *Bioresour. Technol.* 122 (2012) 27–34.
- [7] D.A. Vermaas, D. Kunteng, M. Saakes, K. Nijmeijer, Fouling in reverse electrodialysis under natural conditions, *Water Res.* 47 (2013) 1289–1298.
- [8] J. Moreno, N. de Hart, M. Saakes, K. Nijmeijer, CO₂ saturated water as two-phase flow for fouling control in reverse electrodialysis, *Water Res.* 125 (2017) 23–31.
- [9] S. Pawlowski, C.F. Galinha, J.G. Crespo, S. Velizarov, 2D fluorescence spectroscopy for monitoring ion-exchange membrane based technologies – reverse electrodialysis (RED), *Water Res.* 88 (2016) 184–198.
- [10] J.S. Vrouwenvelder, D.A. Graf von der, J.C. Schulenburg, M.L. Johns Kruihof, M.C.M. van Loosdrecht, Biofouling of spiral-wound nanofiltration and reverse osmosis membranes: a feed spacer problem, *Water Res.* 43 (2009) 583–594.
- [11] R.S. Kingsbury, F. Liu, S. Zhu, C. Boggs, M.D. Armstrong, D.F. Call, O. Coronell, Impact of natural organic matter and inorganic solutes on energy recovery from five real salinity gradients using reverse electrodialysis, *J. Membr. Sci.* 541 (1) (2017) 621–632.
- [12] E.J.M. Kobus, P.M. Heertjes, The poisoning of anion-selective membranes by humic substances, *Desalination* 12 (1973) 333–342.
- [13] E. Korngold, F. de Körösy, R. Rahav, M.F. Taboch, Fouling of anionselective membranes in electrodialysis, *Desalination* 8 (1970) 195–220.
- [14] B. van Berchum, W. van Baak, J. Hessing, Curable compositions and membranes, in: B.V. Europe (Ed.), Fujifilm Manufacturing, Fujifilm Manufacturing Europe BV, The Netherlands, 2011.
- [15] A.H. Galama, D.A. Vermaas, J. Veerman, M. Saakes, H.H.M. Rijnaarts, J.W. Post, K. Nijmeijer, Membrane resistance: the effect of salinity gradients over a cation exchange membrane, *J. Membr. Sci.* 467 (2014) 279–291.
- [16] P. Długołęcki, P. Ogonowski, S.J. Metz, M. Saakes, K. Nijmeijer, M. Wessling, On the resistances of membrane, diffusion boundary layer and double layer in ion exchange membrane transport, *J. Membr. Sci.* 349 (2010) 369–379.
- [17] J. Veerman, M. Saakes, S.J. Metz, G.J. Harmsen, Reverse electrodialysis: a validated process model for design and optimization, *Chem. Eng. J.* 166 (2011) 256–268.
- [18] PCA GmbH, PCA ion exchange membranes technical data sheet, in.
- [19] E.J.M. Kobus, P.M. Heertjes, The poisoning of anion-selective membranes by sodium dodecylsulphate, *Desalination* 10 (1972) 383–401.
- [20] S. Bratskaya, A. Golikov, T. Lutsenko, O. Nesterova, V. Dudarchik, Charge characteristics of humic and fulvic acids: comparative analysis by colloid titration and potentiometric titration with continuous pK-distribution function model, *Chemosphere* 73 (2008) 557–563.
- [21] H.-J. Lee, D.H. Kim, J. Cho, S.-H. Moon, Characterization of anion exchange membranes with natural organic matter (NOM) during electrodialysis, *Desalination* 151 (2003) 43–52.
- [22] S. Pawlowski, T. Rijnaarts, M. Saakes, K. Nijmeijer, J.G. Crespo, S. Velizarov, Improved fluid mixing and power density in reverse electrodialysis stacks with chevron-profiled membranes, *J. Membr. Sci.* 531 (2017) 111–121.